Experimental Cell Research **274,** 100–111 (2002)
doi:10.1006/excr.2001.5460, available online at http://www.idealibrary.com on IDEAL®

Clofibrate-Induced Relocation of Phosphatidylcholine Transfer Protein to Mitochondria in Endothelial Cells

A. P. M. de Brouwer,[1] J. Westerman, A. Kleinnijenhuis, L. E. Bevers, B. Roelofsen, and K. W. A. Wirtz

Department of Biochemistry of Lipids, Institute of Biomembranes, Padualaan 8, 3584 CH Utrecht, The Netherlands

The phosphatidylcholine transfer protein (PC-TP) is a specific transporter of phosphatidylcholine (PC) between membranes. To get more insight into its physiological function, we have studied the localization of PC-TP by microinjection of fluorescently labeled PC-TP in foetal bovine heart endothelial (FBHE) cells and by expression of an enhanced yellow fluorescent protein–PC-TP fusion protein in FBHE cells, human umbilical vein endothelial cells, and HepG2 cells. Analysis by confocal laser scanning microscopy showed that PC-TP was evenly distributed throughout the cytosol with an apparently elevated level in nuclei. By measuring the fluorescence recovery after bleaching it was established that PC-TP is highly mobile throughout the cell, with its transport into the nucleus being hindered by the nuclear envelope. Given the proposed function of PC-TP in lipid metabolism, we have tested a number of compounds (phorbol ester, bombesin, A23187, thrombin, dibutyryl cyclic AMP, oleate, clofibrate, platelet-derived growth factor, epidermal growth factor, and hydrogen peroxide) for their ability to affect intracellular PC-TP distribution. Only clofibrate (100 μM) was found to have an effect, with PC-TP moving to mitochondria within 5 min of stimulation. This relocation did not occur with PC-TP(S110A), lacking the putative protein kinase C (PKC)-dependent phosphorylation site, and was restricted to the primary endothelial cells. Relocation did not occur in HepG2 cells, possibly due to the fact that clofibrate does not induce PKC activation in these cells.

Key Words: **phosphatidylcholine transfer protein; clofibrate; mitochondria; subcellular localization; endothelial cells; FBHE cells; HUVEC; HepG2 cells; PPARα; peroxisome proliferators.**

INTRODUCTION

The phosphatidylcholine transfer protein (PC-TP)[2] is a highly conserved protein (Mw 25 kDa) which specifically transfers phosphatidylcholine (PC) between membranes [1–3]. Although extensive research has been done on the biophysical properties of this protein, little is known about the function of this protein *in vivo*. Possible physiological functions, among which is a role in bile secretion [4, 5], have recently been refuted by van Helvoort *et al.* [3]. In that study, PC-TP null mice failed to give a phenotype. On the other hand, the elucidation of the total genome structure indicated that the promoter region contained a number of responsive elements known to be involved in lipid metabolism [6]. In agreement, PC-TP is particularly expressed in tissues displaying a high lipid turnover, such as liver, kidney, and intestine [3, 7–9].

Although it is generally accepted that PC-TP is primarily present in the cytosol, a proper localization study using immunocytochemistry or immunofluorescence microscopy is lacking. From subfractionation studies it was estimated that about 60% of rat liver PC-TP is present in the cytosolic fraction after subcellular fractionation, the remainder being evenly distributed over the particulate fractions [7]. In the case of the other two major phospholipid transfer proteins in mammals (phosphatidylinositol transfer protein and nonspecific lipid transfer protein), the subcellular localization provided indispensable information about their physiological function (for review see: [10]). In analogy to these proteins, PC-TP could also be involved in specific reactions rather than being a mere transporter of PC from the site of synthesis to the other cellular membranes. If so, such a function may be reflected in a specific subcellular localization.

Here we have investigated the subcellular localization of PC-TP in three different cell lines by microinjection of Oregon Green-labeled PC-TP and by expression of an enhanced yellow fluorescent protein–PC-TP fusion protein (EYFP-PC-TP). Compounds known to affect PC metabolism were tested for their ability to

[1] To whom correspondence and reprint requests should be addressed. Fax: +31-30-2533151. E-mail: a.p.m.debrouwer@chem.uu.nl.

[2] Abbreviations used: CLSM, confocal laser scanning microscopy; DMEM, Dulbecco's modified Eagle's medium; EYFP, enhanced yellow fluorescent protein; PBS, phosphate-buffered saline; nsL-TP, nonspecific lipid transfer protein; PC-TP, phosphatidylcholine transfer protein; PC, phosphatidylcholine; PE, phosphatidylethanolamine; PUFA, polyunsaturated fatty acid; StAR, steroidogenic acute regulatory protein; FBHE, fetal bovine heart endothelial; HUVEC, human umbilical vein endothelial cells.

0014-4827/02 $35.00

influence the subcellular distribution of PC-TP. We show that clofibrate redirects PC-TP to mitochondria in endothelial cells (FBHE cells and HUVEC), but not in HepG2 cells. This relocation is possibly related to phosphorylation of PC-TP.

EXPERIMENTAL PROCEDURES

Materials. FBHE cells were a gift from Mr. J. M. van Aken (Utrecht University, The Netherlands). HUVEC were isolated by Dr. G. Heijnen-Snyder (University Medical Centre Utrecht, The Netherlands). HepG2 cells were a gift from Dr. W. Stoorvogel (University Medical Centre Utrecht, The Netherlands). NIH3T3 mouse fibroblasts were a gift from Dr. P. Meijer, (Hubrecht Laboratorium, The Netherlands). Native PC-TP was isolated from bovine liver as described by Westerman *et al.* [11]. The pEYFP-C1 vector was purchased from Clontech (Palo Alto, CA). The pBluescript SK^- vector and the Quickchange site-directed mutagenesis kit were obtained from Stratagene (La Jolla, CA). Primers were synthesized by Eurogentec (Seraing, Belgium). The FuGENE6 Transfection Reagent Kit was obtained from Roche Molecular Biochemicals (Basel, Switzerland). Ni^{2+}-High Bond matrix was obtained from Invitrogen (San Diego, CA). PD-10 columns were purchased from Amersham Pharmacia Biotech AB (Uppsala, Sweden). The 30- and 100-kDa molecular weight cut-off filters were from Amicon (Beverly, USA). Electroporation cuvettes plus were obtained from Genetronics Inc. (San Diego, CA). G418 (geneticin), egg yolk PC, trinitrophenylphosphatidylethanolamine and phosphatidic acid prepared from egg yolk PC, 5-bromo-4-chloro-3-indoyl-phosphate *p*-toluidine salt, *p*-nitro blue tetrazolium chloride, Coomassie brilliant blue R-250, and goat-anti-rabbit IgG conjugated with alkaline phosphatase were purchased from Sigma (St. Louis, MO). LysoTracker Yellow and MitoTracker Red were obtained from Molecular Probes Europe BV (Leiden, The Netherlands). Antibodies against cytochrome *c* oxidase subunit IV were purchased from Research Diagnostics Inc. (Flanders, USA). Antibodies against the peroxisomal marker nsL-TP labeled with the fluorescent moiety Cy3 were a kind gift from Dr. T. B. Dansen (University Utrecht, The Netherlands). 1-Palmitoyl-, 2-pyrenyl-decanoyl-PC was synthesized according to established procedures and was a kind gift of Dr. P. J. Somerharju (University of Helsinki, Finland). Nonfat dry milk was purchased from Nutricia (Zoetermeer, The Netherlands).

Cell culturing. FBHE cells and HepG2 cells were grown in Dulbecco's modified Eagle's medium (DMEM) containing 10% (v/v) foetal calf serum (FCS) buffered with 44 mM $NaHCO_3$. HUVEC were grown in RPMI-1640 medium containing 20% (v/v) human serum buffered with 44 mM $NaHCO_3$. All cells were maintained at 37°C in a 7.5% CO_2 atmosphere and 95% humidity.

Gel electrophoresis and Western blotting. Cells grown in culture flasks were washed three times with phosphate-buffered saline (PBS; 8.3 mM Na_2HPO_4, 1.5 mM KH_2PO_4, 137 mM NaCl, 2.7 mM KCl, pH 6.9). Total cell lysates were obtained by lysis of the cells in 50 mM Hepes, pH 7.4, 150 mM NaCl, 5 mM EDTA, 0.5% NP-40, 0.5% sodium deoxycholate, 0.1% sodium dodecyl sulfate (SDS), 5 μg/ml leupeptin, 10 mM NaF. Subsequently, proteins were separated by SDS–polyacrylamide gel electrophoresis in 12% acrylamide and 0.37% bis-acrylamide [12] and transferred to a nitrocellulose membrane (Schleicher & Schuell BA 85) by semidry Western blotting in a Multiphor II Nova Blot electrophoretic transfer unit (Pharmacia, Uppsala, Sweden) at 1 mA/cm^2 for 1 h at room temperature. The nonspecific binding sites of the nitrocellulose membrane were blocked by incubating the membrane for 1 h in 2% nonfat dry milk (w/v) in 20 mM Tris–HCl, pH 7.5, 0.5 M NaCl (TBS) at 37°C. Subsequently, the blot was incubated for 1 h at 37°C with the affinity-purified antibody Ab270 raised against native bovine PC-TP [13] diluted 1:20 in TBS containing 0.2% nonfat dry milk (w/v). The blot was washed with TBS–Tween 20 (0.05% v/v) (3× 10 min) and incubated for 1 h with GAR-AP diluted 1:5000 in TBS. The blot was washed again with TBS–Tween 20 (3× 10 min). The immunoreactive proteins were visualized by incubating the blot in 10 ml 0.1 M $NaHCO_3$, pH 9.8, 10 mM $MgCl_2 \cdot 6H_2O$ containing 0.3 mg/ml 5-bromo-4-chloro-3-indoyl-phosphate *p*-toluidine salt and 0.15 mg/ml *p*-nitro blue tetrazolium chloride as the color development substrate.

Oregon Green labeling of PC-TP. Native bovine PC-TP (100 μg) was labeled with a 10-fold molar excess of freshly prepared Oregon Green lodoacetamide 488 in PBS, pH 8.5, in the presence of a 10-fold molar excess of the reducing agent tris-(2-carboxyethyl)phosphine. This mixture was incubated for 48 h under nitrogen at room temperature in the dark. The reaction was stopped by incubation with cysteine (1 μmol) for 30 min at room temperature. Excess label was removed using a PD-10 column equilibrated in PBS, pH 7.4. Labeled protein was concentrated to 400 μg/ml using a 30-kDa molecular weight cut-off filter. By comparing the molar absorbance of the bound fluorophore and of PC-TP, it was estimated that one fluorophore was attached to one molecule of PC-TP. The PC transfer activity was measured according to van Paridon *et al.* [14].

Microinjection of Oregon Green-labeled PC-TP. FBHE cells were grown on glass cover slips to a density of 1×10^4 cells/cm^2. Two days prior to microinjection, the medium was replaced with DMEM containing 10% (v/v) FCS buffered with 20 mM Hepes, pH 7.4. Fluorescently labeled PC-TP (400 μg/ml) was microinjected into the cytosol of FBHE cells by using a combination of an Eppendorf Microinjector (Model 5244) at 90 hPa pressure (approximately 0.2 s) and an Eppendorf Micromanipulator (Model 5170) under an inverted microscope with a 40× air objective. Cells were allowed to recover at 37°C for 1 h. Subsequently, the cells were analyzed by confocal laser scanning microscopy (CLSM).

pEYFP–PC-TP constructs. Bovine PC-TP cDNA [13] was amplified by PCR using the following primers: 5′-cgc aag ctt cga att cc**a tg**g atc ctg ggg ccg gcg cct tc-3′ (sense) and 5′-ctc gaa tcc ggt ac**c ta**g gtt ttc ttg tag ttc tac ga-3′ (antisense). The start and stop codons are printed in boldface. These primers introduce additional *Hin*dIII (sense) and *Kpn*I (antisense) restriction sites (underlined). Using these two enzymes PC-TP was cloned in frame into the pEYFP–C1 vector. Human PC-TP cDNA [3] was cloned into the pEYFP–C1 vector by the same cloning strategy. The primers used were 5′-gcc tcg agc gaa ttc c**at g**ga gct ggc cgc cgg aag-3′ (sense) and 5′-gag gcc ttc ggt acc **tta** ggt ttt ctt gag gta gt-3′ (antisense). The start and stop codons are printed in boldface. These primers introduce additional *Xho*I (sense) and *Kpn*I (antisense) restriction sites (underlined), with which PC-TP was cloned in frame into the pEYFP–C1 vector. Proper insertion of both inserts was checked by restriction analysis and DNA sequencing. In addition, the complete EYFP–PC-TP (bovine and human) open reading frame was cloned into the pET15b vector and expressed in *Escherichia coli*. EYFP–PC-TP was isolated by immobilized metal ion affinity chromatography using Ni^{2+} -High Bond matrix and the transfer activity measured as described above.

Site-directed mutagenesis. Bovine PC-TP cDNA in the pEYFP–C1 vector was subcloned into the pBluescript SK^- vector using *Bam*HI. Using the Quickchange site-directed mutagenesis method Ser^{110} was replaced with Ala. The following primers were used: 5′-cct ttt ccc atg **g**ct aac aga gat tat gtt-3′ (sense) and 5′-aac ata atc tct gtt ag**c** cat ggg aaa agg-3′ (antisense). The boldface nucleotides encode the mutated amino acid (Ser^{110} to Ala) and simultaneously introduce a *Nco*I restriction site (underlined). Incorporation of the changed nucleotides into the construct was checked by restriction enzyme analysis and DNA sequencing. Subsequently, the mutated PC-TP(S110A) was cloned back into the pEYFP–C1 vector using *Bam*HI and the orientation checked by restriction analysis. Bovine PC-TP(S110A) was also expressed in *E. coli* using the pET15b expression vector. The PC transfer activity in the bacterial cytosol was measured as described above.

Transfection. FBHE cells and HepG2 cells were transfected by lipofection. Cells were seeded at 1×10^4 cells/cm^2 on glass cover slips. After 24 h of growth, cells were transfected with 1 μg of the pEYFP–PC-TP vector using the FuGENE6 Transfection Reagent Kit according to the instruction of the manufacturer and after 24 h were analyzed by CLSM. HUVEC were transfected by electroporation. Cells were seeded at 2×10^4 cells/cm^2 in a 75-cm^2 flask. After 24 h of growth, the medium was removed and the cells were washed two times with PBS. Then 0.25% Trypsin–0.03% EDTA (w/w) (1 ml) in PBS was added and the flask incubated at 37°C until the cells detached. Next, 5 ml RPMI medium containing 20% human serum was added and the cells were centrifuged at 100*g* for 5 min. The cells were resuspended in 2 ml PBS and centrifuged again at 100*g* for 5 min. Subsequently, cells were resuspended in 0.8 ml PBS. DNA (4 μg) was added and the suspension was transferred into a 4-mm-gap electroporation cuvette plus. Cells were subjected to two pulses of 0.3 ms with a capacity of 25 μF and a voltage of 850 V using a Bio-Rad Gene pulser II (Bio-Rad Laboratories, Hercules, CA). Subsequently, 10 ml RPMI containing 20% human serum was added and the cells were left to recuperate for 24 h under normal conditions on glass cover slips.

Stimulation of cells. Cells containing EYFP–PC-TP or Oregon Green-labeled PC-TP were grown to a density of 2×10^4 cells/cm^2 on glass coverslips and stimulated by fresh serum-free medium containing clofibrate and other agonists for different periods of time (0–120 min). The cells were fixed with 4% paraformaldehyde in PBS and the distribution of fluorescence was analyzed by CLSM. In some instances, fluorescence was determined by *in vivo* imaging up to 30 min.

Identification of subcellular organelles. Cells were washed two times with PBS and fixed by incubation in 4% paraformaldehyde in PBS for 1 h at 37°C. Fixed cells were permeabilized by 0.5% Triton X-100 in PBS (5 min) and subsequently washed two times for 5 min in 50 mM NH_4Cl in PBS. Prior to labeling with antibodies, nonspecific binding sites were blocked with 2 mg/ml gelatine in PBS for 1 h. Peroxisomes were identified by Cy3-labeled antibodies directed against the nsL-TP [15] and mitochondria by TRITC-labeled antibodies against cytochrome *c* oxidase subunit IV. The coverslips were mounted in 20 mM Tris–HCl, pH 8.5, 24% Gelvatol 4-88, 6% glycerol. Mitochondria and lysosomes were identified in living cells by addition of serum-free medium containing 50 μM MitoTracker Red or LysoTracker Yellow.

Confocal laser scanning microscopy. Fluorescence was visualized by confocal laser scanning microscopy using a Leica TCSNT confocal laser scanning microscope on an inverted microscope DMIRBE (Leica Microsystems, GmbH, Heidelberg, Germany) with an argon–krypton laser as excitation source. In the case of the Oregon Green 488 and EYFP, $\lambda_{excitation}$ and $\lambda_{emission}$ were 488 and 530 nm $\pm$ 15 nm, respectively. In the case of Cy3, TRITC, MitoTracker Red, and LysoTracker Yellow, $\lambda_{excitation}$ and $\lambda_{emission}$ were 568 and 600 nm $\pm$ 15 nm, respectively. Overlap from the green into the red channel and vice versa was checked before recording the images and, if necessary, corrected.

Bleaching. To bleach the fluorescently labeled PC-TP in cells, a distinct section of the cytosol or the nucleus was scanned 16 times with the pinhole set at maximum depth. Immediately after bleaching, settings were returned to normal and the remainder of the fluorescence was visualized. To quantify the recovery after bleaching, the fluorescence intensity of each pixel in a part of the nucleus (2000 pixels) and the cytosol (14,000 pixels) was determined at various time points and the fraction of fluorescence present in the nucleus calculated.

Correlation plots. Correlation plots were generated using the plotting macro provided with Scion Image release Beta 3b.

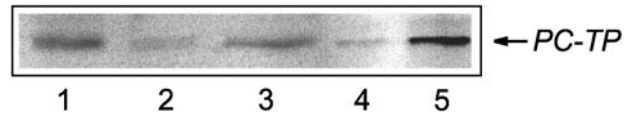

FIG. 1. Immunoblot analysis of PC-TP in total cell lysates. Lane 1, HepG2 cells (20 μg protein); lane 2, HUVEC (150 μg protein); lane 3, FBHE cells (25 μg protein); lane 4, native bovine PC-TP (10 ng); lane 5, native bovine PC-TP (30 ng).

RESULTS

PC-TP Levels and Subcellular Localization

The subcellular localization of PC-TP was investigated in three different cell lines, i.e. FBHE cells, HUVEC, and HepG2 cells. As established by densitometric scanning of immunoblots, it was estimated that FBHE cells, HUVEC, and HepG2 cells contain 1.0, 0.1, and 3.4 μg PC-TP/mg total protein, respectively (Fig. 1). Affinity-purified polyclonal antibodies raised against bovine liver PC-TP were used to determine the intracellular distribution of PC-TP in these cells. However, when prior to use the specific antibodies were removed by incubation with pure native bovine PC-TP, nonspecific staining was still clearly visible (results not shown). These nonspecific interactions prevented the use of the polyclonal antibody in the immunolocalization. Hence, the subcellular localization was determined by the microinjection of bovine PC-TP labeled with Oregon Green 488 and by the expression of an enhanced yellow fluorescent protein–PC-TP fusion protein. Fluorescent tagging of PC-TP had no effect on the PC transfer activity (data not shown). The CLSM images in Fig. 2 show the localization of PC-TP in the equatorial plane. In the case of FBHE cells the Oregon Green-labeled PC-TP and the EYFP–bovine PC-TP were found throughout the cytosol with elevated levels present in the nucleus (Figs. 2A and 2B). When EYFP–human PC-TP was expressed in HUVEC or HepG2 cells, the same localization was observed (Figs. 2C and 2D). Since pure human PC-TP was not available, the localization studies of these cells were restricted to the fusion protein. Expression of EYFP in all three cell lines gave a similar distribution, indicating that the enrichment of PC-TP in the nucleus was not an inherent property of this protein (Figs. 2E–2G).

Intracellular Mobility

To investigate the mobility of Oregon Green-labeled PC-TP in the cell, the fluorophore was bleached in a distinct section of either the nucleus or the cytosol, and the recovery of fluorescence was measured. Bleaching a section of the nucleus diminished the fluorescence intensity of the complete nucleus (Fig. 3). After bleaching, the fluorescence intensity was restored to virtually

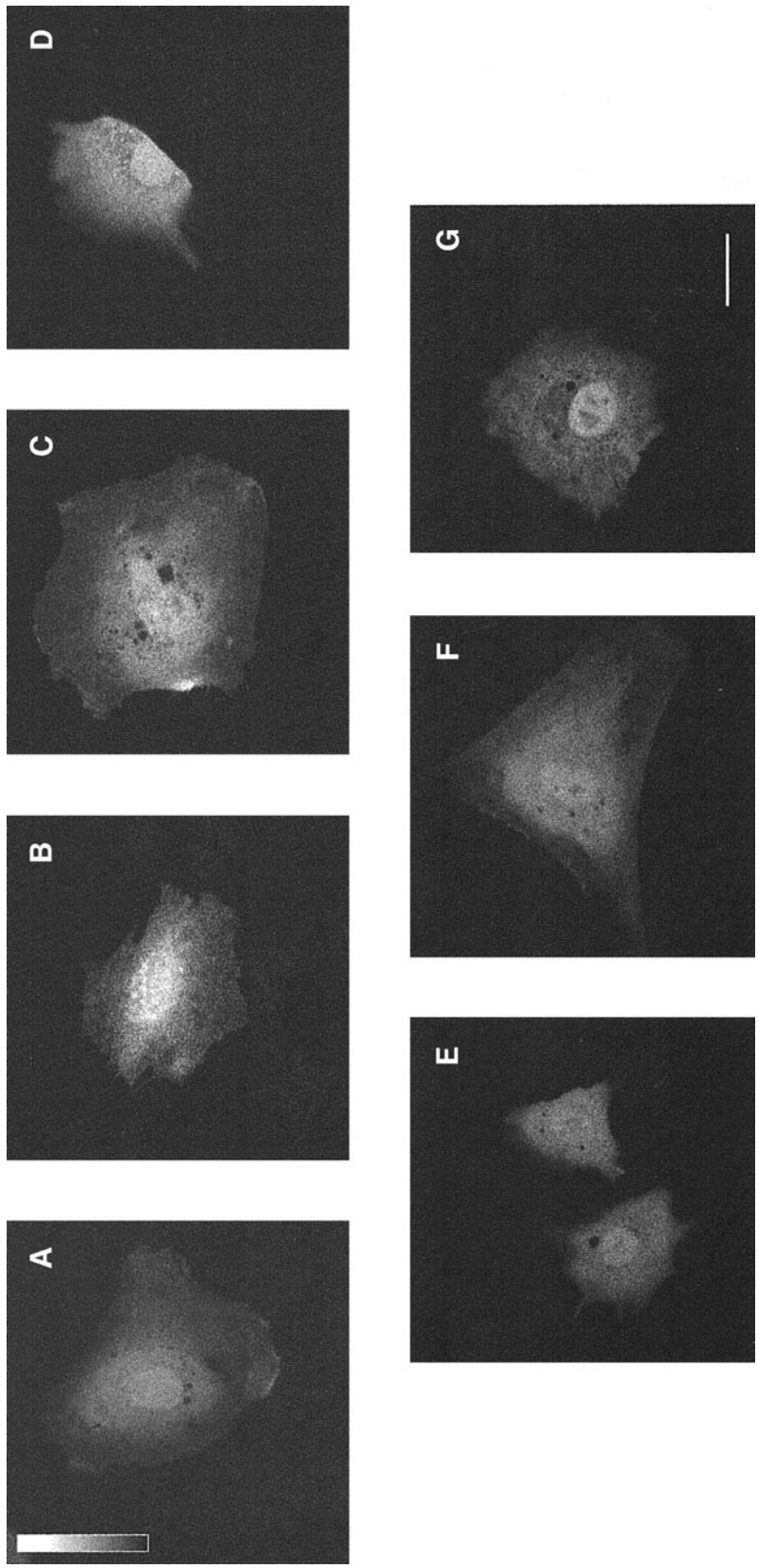

FIG. 2. Subcellular distribution of PC-TP. (A) Oregon Green-labeled PC-TP microinjected into FBHE cells; (B–D) EYFP–PC-TP expressed in FBHE cells, HUVEC, and HepG2 cells; (E–G), EYFP expressed in FBHE cells, HUVEC, and HepG2 cells. Inset shows the intensity from high (white) to low (black); the bar represents a length of 20 μm. Images were obtained by confocal laser scanning microscopy.

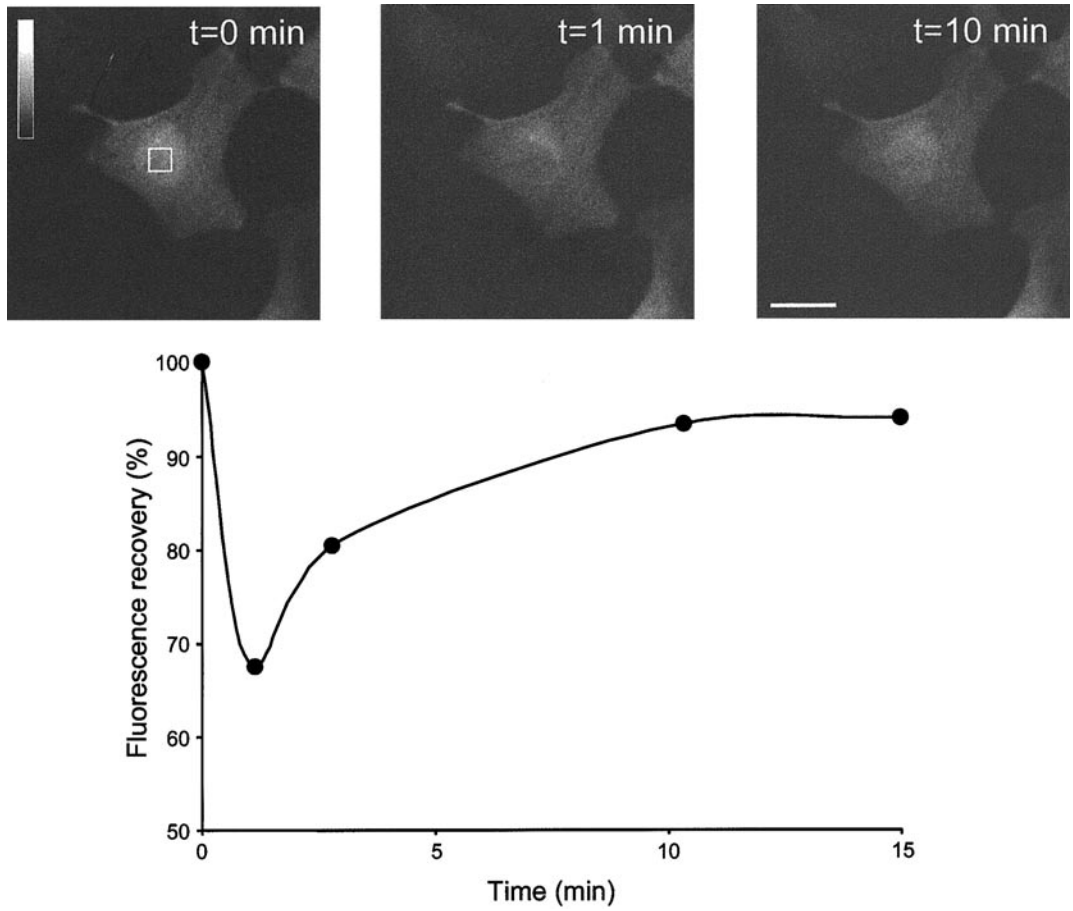

FIG. 3. Fluorescence recovery after bleaching of Oregon Green-labeled PC-TP in the nucleus of FBHE cells. Top: distribution of PC-TP at different time points. The white square indicates the bleached area in the nucleus. Inset shows the intensity from high (white) to low (black); the bar represents a length of 20 μm. Images were obtained by confocal laser scanning microscopy. Bottom: quantification of fluorescence recovery.

the initial level within 10 min. The time course of recovery after bleaching in the nucleus is shown in Fig. 3 (bottom). In the case of bleaching a section of the cytosol, the fluorescence recovery was instantaneous (less than 30 s). This indicates that PC-TP can move freely throughout the cell; yet the movement across the nuclear membrane is restricted. Similar results were obtained by bleaching EYFP–PC-TP in FHBE cells, HUVEC, and HepG2 cells. In the case of the EYFP fusion proteins, the fluorescence recovery in the nucleus was approximately 15 min (data not shown).

Clofibrate-Induced Relocation to Mitochondria

With PC-TP being able to move freely through the cell, it can deliver PC to specific sites of metabolism or to distinct membrane domains in need of PC. To obtain evidence for this, FBHE cells microinjected with Oregon Green-labeled PC-TP were stimulated with compounds that affect PC hydrolysis or synthesis. The compounds tested were phorbol ester (50 and 100 ng/ml), bombesin (10 nM), A23187 (1 and 4 μg/ml), thrombin (0.1 and 1 U/ml), dibutyryl cyclic AMP (1 mM), oleate (0.5 and 2 mM), clofibrate (100, 200, and 500 μM), lysophosphatidic acid (10 μg/ml), tumor necrosis factor (1 and 50 ng/ml), platelet-derived growth factor (20 ng/ml), epidermal growth factor (50 ng/ml), and hydrogen peroxide (200 μM). None of these compounds influenced the distribution of fluorescently labeled PC-TP (data not shown). An exception, however, was clofibrate, an inhibitor of the PE methylation pathway, which caused an extensive redistribution of PC-TP within 5 min (Fig. 4). PC-TP remained associated with distinct cellular structures up to 25 min. As a control, Oregon Green-labeled bovine serum albumin was injected into FBHE cells. The distribution of this protein was not affected by clofibrate treatment (data not shown).

Since clofibrate primarily influences the function of peroxisomes [16, 17] and mitochondria [18–20], attention was focused on these two organelles as possible

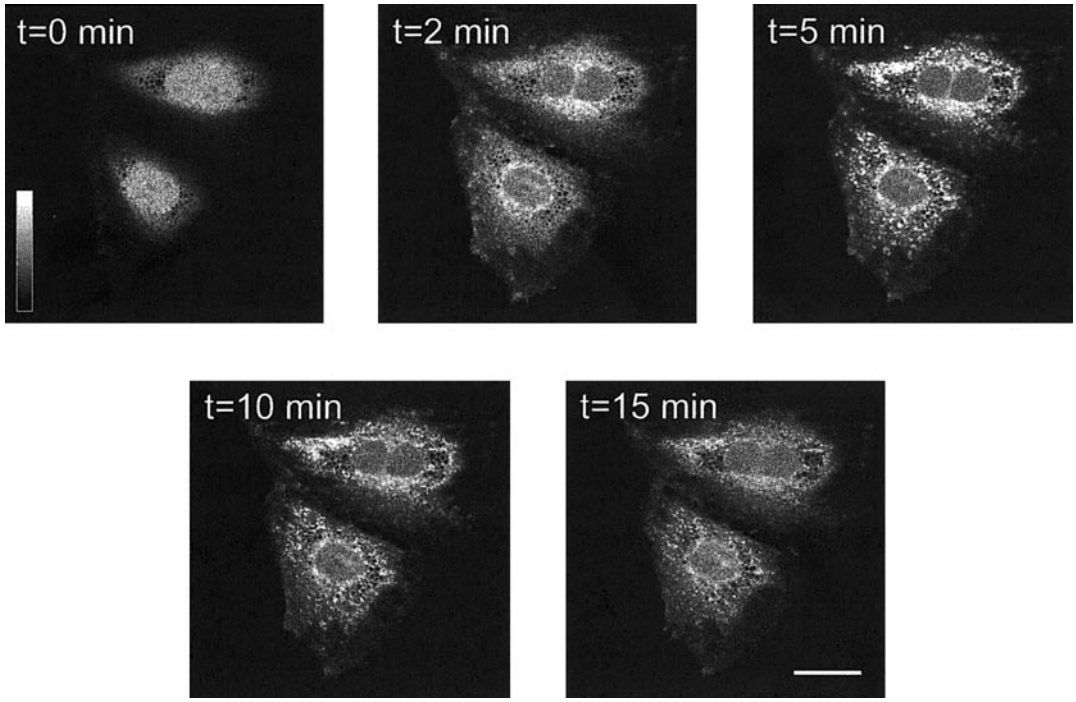

FIG. 4. Distribution of Oregon Green-labeled PC-TP in FBHE cells as a function of time after stimulation with clofibrate (100 μM). Inset shows the intensity from high (white) to low (black); the bar represents a length of 20 μm. Images were obtained by confocal laser scanning microscopy.

sites of interaction for PC-TP. To be sure that labeling of these structures did not indicate sites of enhanced degradation of PC-TP, lysosomes were also taken into consideration. After a 5-min stimulation by clofibrate and fixation of the FBHE cells, PC-TP did not colocalize with antibodies directed against nsL-TP, a peroxisomal protein (Fig. 5A). Using a lysosomal marker (LysoTracker Yellow) during *in vivo* imaging, it was demonstrated that the PC-TP-associated structures were not lysosomes (Fig. 5B). However, a distinct colocalization was observed with MitoTracker Red (also measured *in vivo*), indicating that PC-TP is associated with mitochondria after clofibrate stimulation (Fig. 5C). This colocalization was confirmed by computing the correlation between the red and the green channels. By superimposing the two images the intensity of each separate pixel was compared (Fig. 6). The correlation coefficient between MitoTracker Red and PC-TP after relocation was 0.92, whereas the correlation coefficients for peroxisomes and lysosomes were 0.56 and 0.54, respectively.

The relocation was also investigated for EYFP–PC-TP expressed in FBHE cells, HUVEC, and HepG2 after administration of 100 μM clofibrate. After stimulation and fixation of the cells, the mitochondria were stained by antibodies directed against cytochrome *c* oxidase subunit IV. In both FBHE cells and HUVEC, EYFP–PC-TP was associated with mitochondria (Figs. 7A and 7B). However, it can be seen that not all mitochondria show PC-TP labeling, strongly suggesting that PC-TP has relocated to a subset of mitochondria (see insets). The occurrence of two populations of mitochondria is reflected in the relatively low correlation coefficients of 0.82 for FBHE cells and 0.65 for HUVEC (Fig. 8). No relocation to mitochondria was observed for the HepG2 cells (data not shown). EYFP expressed in these cells did not relocate to mitochondria in response to clofibrate treatment. In addition to clofibrate, arachidonic acid (500 μM) was observed to induce mitochondrial relocation of EYFP–PC-TP in FBHE cells and HUVEC (results not shown).

Relocation Is Associated with the PKC Phosphorylation Site at Serine-110

PC-TP has one putative PKC phosphorylation site at Ser^{110} [21–23]. Ser^{110} is the structural homologue of Ser^{195} in steroid acute regulatory protein (StAR) [24]. Upon phosphorylation StAR moves to mitochondria to deliver cholesterol to the mitochondrial membrane. Since the same mechanism might apply for PC-TP, Ser^{110} was replaced for an alanine residue by site-directed mutagenesis. After expression in *E. coli* the mutated bovine protein denoted PC-TP(S110A) was fully active compared to nonmutated bovine PC-TP (data not shown). Upon expression of the EYFP–PC-

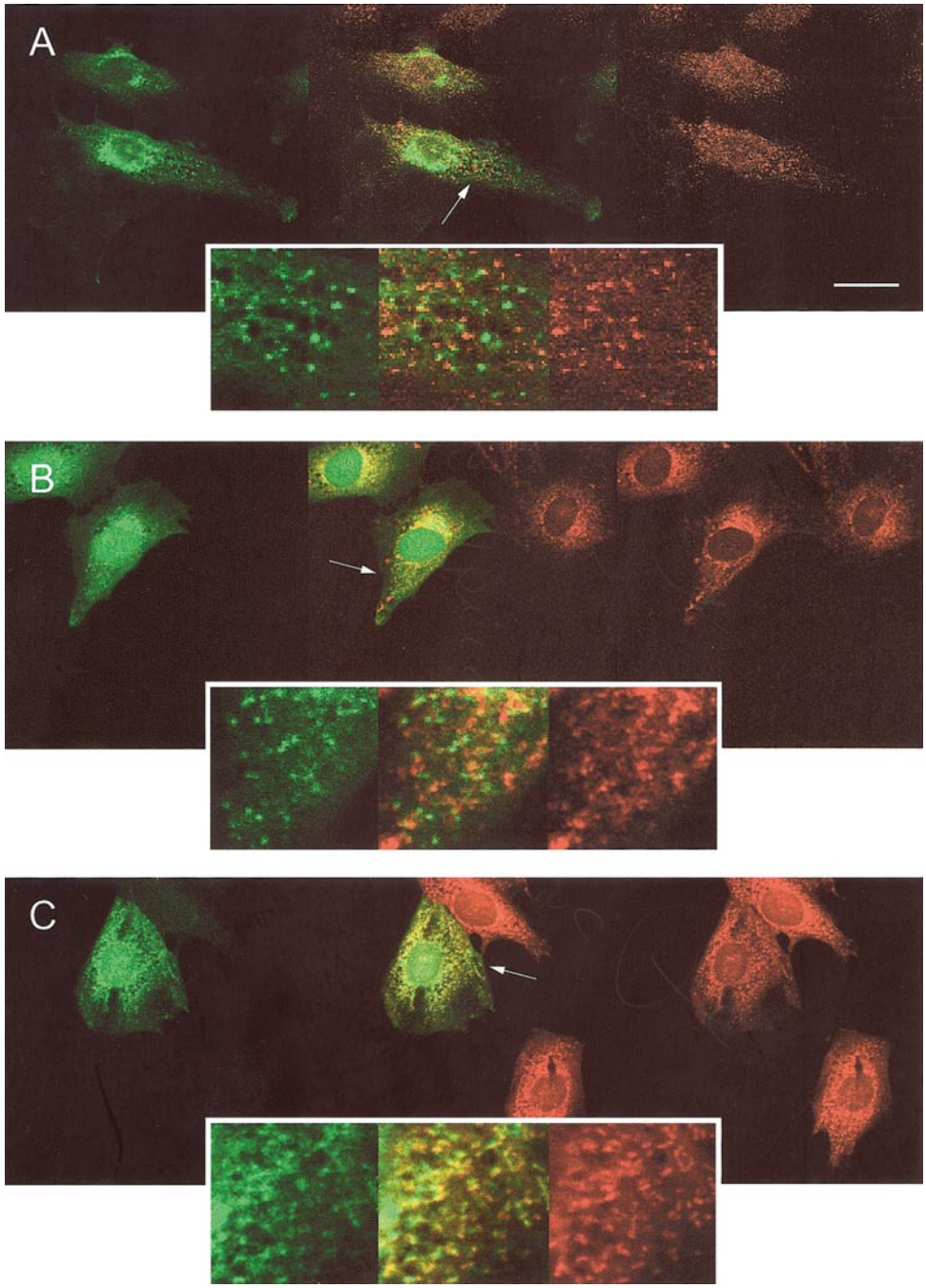

FIG. 5. Mitochondrial localization of Oregon Green-labeled PC-TP in FBHE cells after stimulation with clofibrate. PC-TP is shown on the left and markers for peroxisomes (A), lysosomes (B), and mitochondria (C) on the right. The middle image of each panel shows the colocalization as indicated by the yellow color. Peroxisomes were identified by Cy3-labeled antibodies directed against nsL-TP, lysosomes by LysoTracker Yellow, and mitochondria by MitoTracker Red. Arrows point to the segment of the cell corresponding with the inset. The bar represents a length of 20 μm. All images were obtained by confocal laser scanning microscopy.

TP(S110A) fusion protein in FBHE cells, 100 μM clofibrate did not induce relocation to the mitochondria (Fig. 9A), whereas EYFP–PC-TP used as control did relocate (Fig. 9B). This strongly suggests that clofibrate-induced relocation to the mitochondria is associated with phosphorylation of Ser^{110}.

DISCUSSION

Despite numerous efforts, the physiological function of the highly conserved PC-TP still remains to be established [3]. Here we show by confocal laser scanning microscopy that fluorescently labeled PC-TP was

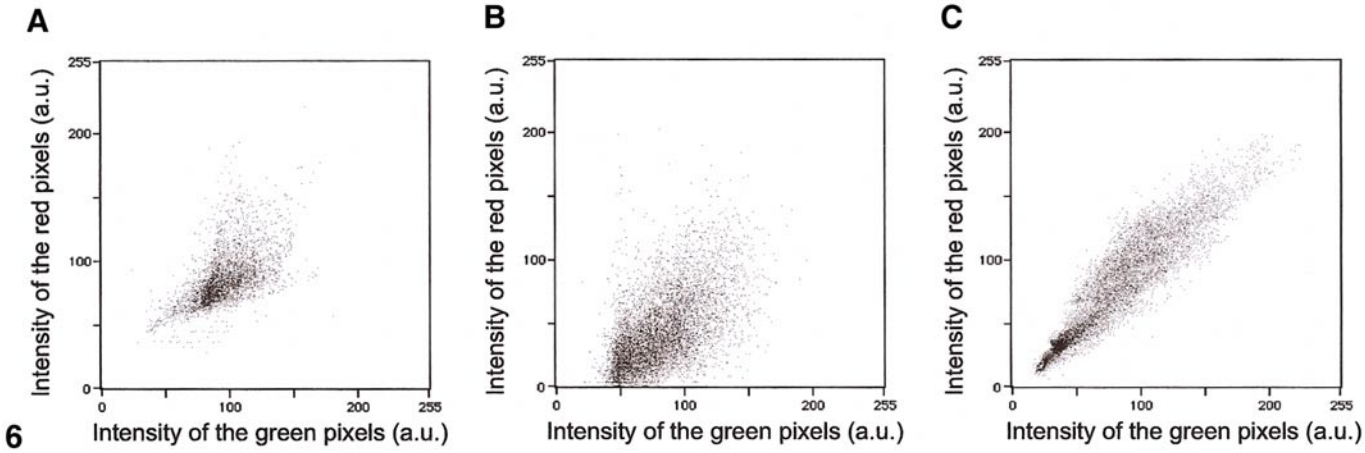

6

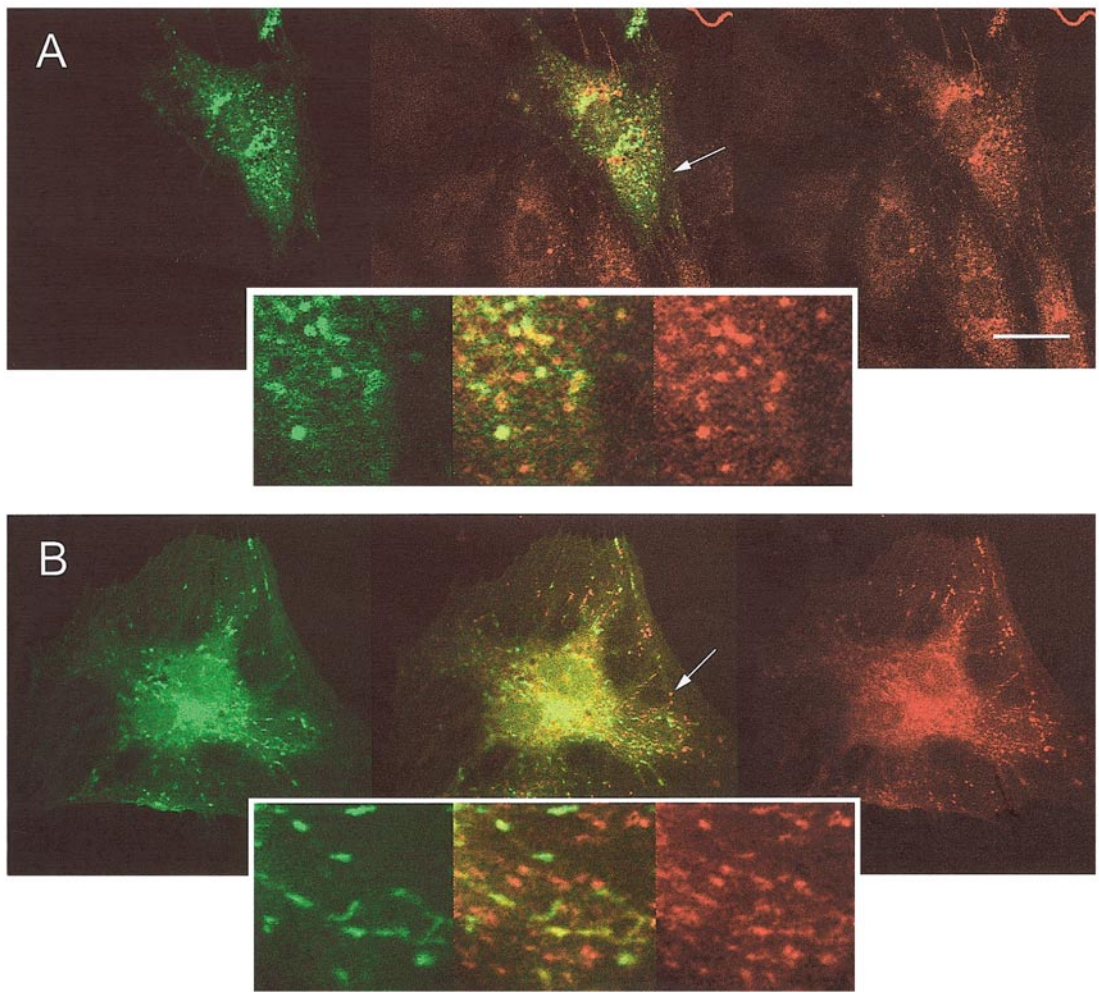

7

FIG. 6. Correlation plots of the subcellular distribution of PC-TP and markers of peroxisomes (A), lysosomes (B), and mitochondria (C) in FBHE cells after stimulation with clofibrate. The intensity of each pixel in the green and red channel is determined and plotted against each other. The derived correlation coefficients are 0.56 for peroxisomes, 0.54 for lysosomes, and 0.92 for mitochondria. A correlation coefficient of 1.0 indicates complete colocalization and a value of 0.5 no colocalization of PC-TP and marker.

FIG. 7. Mitochondrial localization of EYFP–PC-TP after stimulation with clofibrate in FBHE cells (A) and HUVEC (B). On the left side of each panel the green channel (PC-TP) is shown and on the right side the red channel (mitochondria). The middle image of each panel shows the colocalization as indicated by the yellow color. Mitochondria were identified using antibodies directed against TRITC-labeled cytochrome *c* oxidase subunit IV. Arrows point to the segment of the cell corresponding with the inset. The bar represents a length of 20 μm. All images were obtained by confocal laser scanning microscopy.

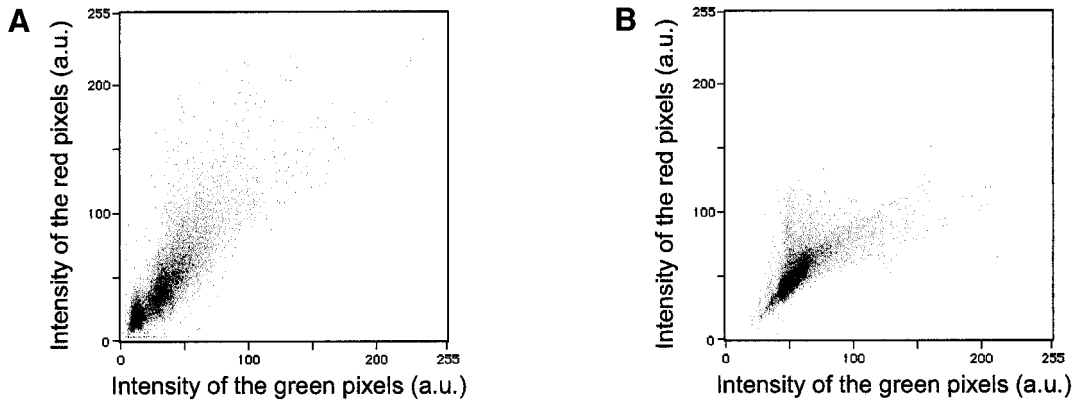

FIG. 8. Correlation plots comparing the colocalization of EYFP–PC-TP with a mitochondrial marker in FBHE cells (A) and HUVEC (B) after stimulation with clofibrate. The derived correlation coefficients are 0.82 for FBHE cells and 0.65 for HUVEC. The relatively low correlation coefficients reflect the association of PC-TP with a subset of mitochondria (see legend to Fig. 6).

evenly distributed throughout the cytoplasm of FBHE cells, HUVEC, and HepG2 cells with elevated levels in the nuclei. This latter enrichment was also observed for EYFP expression in these cells, which argues against a specific function for PC-TP in the nuclei. By fluorescence recovery after bleaching PC-TP was found to be highly mobile throughout the cell. Bleaching of PC-TP in the nuclei indicated that the mobility of PC-TP between the cytosol and the nucleus was restricted, requiring a recovery period of 10 min for Oregon Green-labeled PC-TP and 15 min for EYFP–PC-TP. Similar times of recovery have been observed after the nuclear bleaching of fluorescently labeled dextrans having the same size [25–27].

Addition of clofibrate (100 μM) to the medium of endothelial cells caused PC-TP to move to mitochondria within 5 min. Another peroxisome proliferator, arachidonic acid (500 μM), could also induce this relocation (data not shown). Peroxisome proliferators induce phosphorylation of serine and threonine residues by protein kinase C (PKC) [28–35]. These modifications appear to be either an early event or a mechanism independent of peroxisome proliferation. When we substitute Ser^{110}, which is part of a putative PKC phosphorylation site for an alanine residue, the relocation of PC-TP is abolished. This strongly suggests that the clofibrate-induced relocation of PC-TP to the mitochondria is preceded by PKC phosphorylation. The PKC isoform involved is probably specific, since rat brain PKC consisting mainly of PKCγ was not able to phosphorylate PC-TP for more than 0.2% *in vitro* (data not shown). Clofibrate was unable to induce the relocation of EYFP–PC-TP in HepG2 cells. This agrees with fibrates not being able to induce phosphorylation in these cells [32]. The specific relocation of PC-TP to mitochondria upon phosphorylation strongly suggests

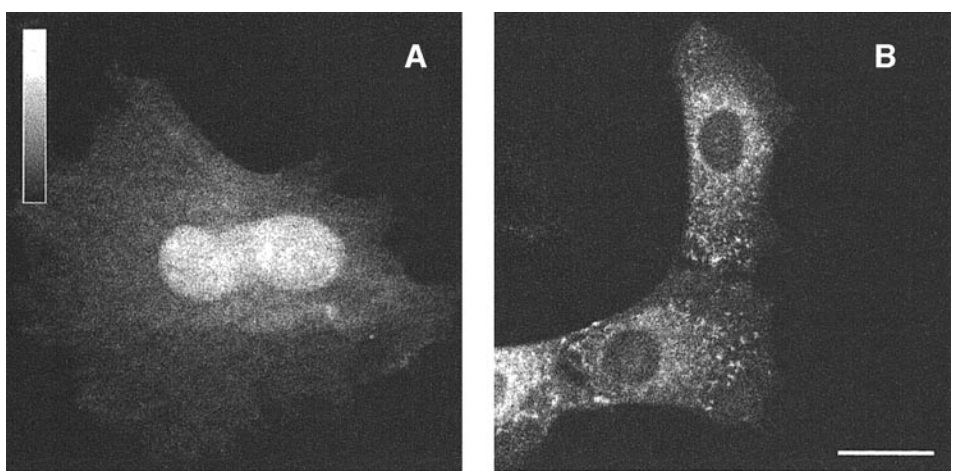

FIG. 9. Effect of the replacement of Ser^{110} with Ala on the distribution of PC-TP in FBHE cells after stimulation with clofibrate (200 μM). (A) EYFP–PC-TP(S110A); (B) EYFP–PC-TP.

that mitochondria contain docking proteins, which interact with the phosphorylated PC-TP. After docking, PC-TP most likely stays on the outside of the mitochondria, since PC-TP does not contain a mitochondrial localization signal [36].

Clofibrate is an inhibitor of PE methyltransferase (PEMT) mediating the methylation of PE to PC, a process that takes place in the mitochondria-associated membranes [37, 38]. Inhibition of PEMT impairs the lipidation of apolipoprotein B48-containing lipoproteins, leading to decreased triglyceride (TG) and phospholipid levels in blood [39]. Interestingly, clofibrate treatment did not affect blood plasma TG and phospholipid levels in PC-TP null mice (A. P. M. de Brouwer *et al.*, unpublished). In view of its association with mitochondria after clofibrate stimulation, we consider the possibility that the clofibrate-mediated inhibition of PEMT is linked to PC-TP translocation. In line with this, PC-TP is not relocated in HepG2 cells, which display very low PEMT activity [40]. On the other hand, the PE methylation pathway appears to be restricted to liver [41], whereas PC-TP is more ubiquitously expressed.

In transferring PC between membranes, PC-TP prefers PC molecular species that have a palmitic acid on the *sn*-1 position and polyunsaturated fatty acid (PUFA) on the *sn*-2 position [42]. It is conceivable that relocation of PC-TP to mitochondria increases the amount of 16:0/PUFA-PC species in the mitochondrial membranes. The ensuing increase of membrane fluidity is reported to generate a number of responses, such as the enhancement of membrane-associated phospholipase A_2 activity [43], proton leakage [44, 45], and Ca^{2+} efflux [46]. Furthermore, changes in phospholipid fatty acid composition can alter the activity of carnitine palmitoyltransferase I [47, 48] and of the pyruvate carrier [49, 50]. If correct, the interaction of PC-TP with mitochondria may have a profound effect on mitochondrial function, including an increased β-oxidation. In this regard it is to be noted that fibrates exert their hypotriglyceridemic effect primarily via increased β-oxidation in the mitochondria [51].

Although many implications resulting from the relocation of PC-TP to mitochondria can be envisaged, we have as yet no direct proof that PC-TP regulates mitochondrial function. However, given that clofibrate treatment both induces relocation of PC-TP to the mitochondria and stimulates a PC-TP-mediated decrease in blood plasma TG and phospholipid levels, it is evident that attention should be focused on PC-TP in connection to mitochondrial lipid metabolism.

We thank Dr. G. J. P. L. Kops (Physiological Biochemistry, UMC Utrecht, The Netherlands), Dr. W. J. Hage (Hubrecht Laboratorium, The Netherlands), and Dr. C. A. M. de Haan (Infectious diseases and Immunology, Utrecht University, The Netherlands) for their assistance with the microinjection experiments, confocal laser scanning microscopy, and electroporation, respectively.

REFERENCES

1. Kamp, H. H., Wirtz, K. W. A., Baer, P. R., Slotboom, A. J., Rosenthal, A. F., Paltauf, F., and van Deenen, L. L. M. (1977). Specificity of the phosphatidylcholine exchange protein from bovine liver. *Biochemistry* **16,** 1310–1316.
2. Moonen, P., Akeroyd, R., Westerman, J., Puijk, W. C., Smits, P., and Wirtz, K. W. A. (1980). The primary structure of the phosphatidylcholine-exchange protein from bovine liver. *Eur. J. Biochem.* **106,** 279–290.
3. van Helvoort, A., de Brouwer, A. P. M., Ottenhof, R., Brouwers, J. F. H. M., Brouwers, Wijnholds, J., Beijnen, J. H., Rijneveld, A., van der Poll, T., van der Valk, M. A., Majoor, D., Voorhout, W., Wirtz, K. W. A., Oude Elferink, R. P. J., and Borst, P. (1999). Mice without phosphatidylcholine transfer protein have no defects in the secretion of phosphatidylcholine into bile or into lung airspaces. *Proc. Natl. Acad. Sci. USA* **96,** 11501–11506.
4. Cohen, D. E., Leonard, M. R., and Carey, M. C. (1994). *In vitro* evidence that phospholipid secretion into bile may be coordinated intracellularly by the combined actions of bile salts and the specific phosphatidylcholine transfer protein of liver. *Biochemistry* **33,** 9975–9980.
5. LaMorte, W. W., Booker, M. L., and Kay, S. (1998). Determinants of the selection of phosphatidylcholine molecular species for secretion into bile of the rat. *Hepatology* **28,** 631–637.
6. Wu, M. K., Boylan, M. O., and Cohen, D. E. (1999). Cloning and gene structure of rat phosphatidylcholine transfer protein. *Gene* **235,** 110–120.
7. Teerlink, T., Van der Krift, T. P., Post, M., and Wirtz, K. W. A. (1982). Tissue distribution and subcellular localization of phosphatidylcholine transfer protein in rats as determined by radioimmunoassay. *Biochim. Biophys. Acta* **713,** 61–67.
8. Geijtenbeek, T. B. H., Smith, A. J., Borst, P., and Wirtz, K. W. A. (1996). cDNA cloning and tissue-specific expression of the phosphatidylcholine transfer protein gene. *Biochem. J.* **316,** 49–55.
9. Cohen, D. E., Green, R. M., Wu, M. K., and Beier, D. R. (1999). Cloning, tissue-specific expression, gene structure and chromosomal localization of human phosphatidylcholine transfer protein. *Biochim. Biophys. Acta* **1447,** 265–270.
10. Wirtz, K. W. A. (1997). Phospholipid transfer proteins revisited. *Biochem. J.* **324,** 353–360.
11. Westerman, J., Kamp, H. H., and Wirtz, K. W. A. (1983). Phosphatidylcholine transfer protein from bovine liver. *Methods Enzymol.* **98,** 581–586.
12. Snoek, G. T., de Wit, I. S. C., van Mourik, J. H. G., and Wirtz, K. W. A. (1992). The phosphatidylinositol transfer protein in 3T3 mouse fibroblast cells is associated with the Golgi system. *J. Cell. Biochem.* **49,** 339–348.
13. de Brouwer, A. P. M., Bouma, B., van Tiel, C. M., Heerma, W., Brouwers, J. F. H. M., Bevers, L. E., Westerman, J., Roelofsen, B., and Wirtz, K. W. A. (2001). The binding of phosphatidylcholine to the phosphatidylcholine transfer protein: Affinity and role in folding. *Chem. Phys. Lipids* **112,** 109–119.
14. van Paridon, P. A., Visser, A. J. W. G., and Wirtz, K. W. A. (1987). Binding of phospholipids to the phosphoinositol transfer protein from bovine brain as studied by steady-state and time-resolved fluorescence spectroscopy. *Biochim. Biophys. Acta* **898,** 172–180.
15. Ossendorp, B. C., Voorhout, W., van Amerongen, A., Brunnik, F., Batenburg, J. J., and Wirtz, K. W. A. (1996). Tissue-specific

distribution of a peroxisomal 46-kDa protein related to the 58-kDa protein (sterol carrier protein x; sterol carrier protein 2/3-oxoacyl–CoA thiolase). *Arch. Biochem. Biophys.* **334,** 251–260.

16. Rusyn, I., Rose, M. L., Bojes, H. K., and Thurman, R. G. (2000). Novel role of oxidants in the molecular mechanism of action of peroxisome proliferators. *Antioxid. Redox. Signal.* **2,** 607–621.
17. Dzhekova-Stojkova, S., Bogdanska, J., and Stojkova, Z. (2001). Peroxisome proliferators: Their biological and toxicological effects. *Clin. Chem. Lab. Med.* **39,** 468–474.
18. Hakkola, E. H., Hiltunen, J. K., and Autoio-Harmainen H. I. (1994). Mitochondrial 2,4-dienoyl–CoA reductase in the rat: Differential responses to clofibrate treatment. *J. Lipid Res.* **35,** 1820–1828.
19. Qu, B., Li, Q.-T., Wong, W. P., Ong, C., N., and Halliwell, D. (1999). Mitochondrial damage by the 'pro-oxidant' peroxisomal proliferator clofibrate. *Free Radic. Biol. Med.* **27,** 1095–1102.
20. Zhou, S., and Wallace, K. B. (1999). The effect of peroxisome proliferators on mitochondrial bioenergetics. *Toxicol. Sci.* **48,** 82–89.
21. Kishimoto, A., Nishiyama, K., Nakanishi, H., Uratsuji, Y., Nomura, H., Takeyama, Y., and Nishizuka, Y. (1985). Studies on the phosphorylation of myelin basic protein by protein kinase C and adenosine 3′:5′-monophosphate-dependent protein kinase. *J. Biol. Chem.* **260,** 12492–12499.
22. Woodgett, J. R., Gould, K. L., and Hunter, T. (1986). Substrate specificity of protein kinase C. Use of synthetic peptides corresponding to physiological sites as probes for substrate recognition requirements. *Eur. J. Biochem.* **161,** 177–184.
23. Nishikawa, K., Toker, A., Johannes, F-J., Songyang, Z., and Cantley, L. C. (1997). Determination of the specific substrate sequence motifs of protein kinase C isozymes. *J. Biol. Chem.* **272,** 952–960.
24. Tsujishita, Y., and Hurley, J. H. (2000). Structure and lipid transport mechanism of a StAR-related domain. *Nat. Struct. Biol.* **7,** 408–414.
25. Peters, R. (1983). Nuclear envelope permeability measured by fluorescence microphotolysis of single liver cell nuclei. *J. Biol. Chem.* **258,** 11427–11429.
26. Peters, R. (1984). Nucleo-cytoplasmic flux and intracellular mobility in single hepatocytes measured by fluorescence microphotolysis. *EMBO J.* **3,** 1831–1836.
27. Lang, I., Scholz, M., and Peters, R. (1986). Molecular mobility and nucleocytoplasmic flux in hepatoma cells. *J. Cell Biol.* **102,** 1183–1190.
28. Bojes, H. K., Keller, B. J., and Thurman, R. G. (1992). Wy-14643 stimulates hepatic protein kinase C activity. *Toxicol. Lett.* **62,** 317–322.
29. Watanabe, T., Okawa, S., Itoga, H., Imaka, T., and Suga, T. (1992). Involvement of calmodulin- and protein kinase C-related mechanism in an induction process of peroxisomal fatty acid oxidation-related enzymes by hypolipidemic peroxisome proliferators. *Biochim. Biophys. Acta* **1135,** 84–90.
30. Bojes, H. K., and Thurman, R. G. (1994). Peroxisome proliferators inhibit acyl–CoA synthase and stimulate protein kinase C *in vivo*. *Toxicol. Appl. Pharmacol.* **126,** 233–239.
31. Leibold, E., Greim, H., and Schwarz, L. R. (1994). Inhibition of intercellular communication of rat hepatocytes by nafenopin-involvement of protein kinase *C. Carcinogenesis* **15,** 1265–1269.
32. Passilly, P., Jannin, B., and Latruffe, N. (1995). Influence of peroxisome proliferators on phosphoprotein levels in human and rat hepatic-derived cell lines. *Eur. J. Biochem.* **230,** 316–321.
33. Motojima, K., Passilly, P., Jannin, B., and Latruffe, N. (1996). Protein phosphorylation by peroxisome proliferators: Species-specific stimulation of protein kinases. *Ann. N. Y. Acad. Sci.* **804,** 413–423.
34. Rokos, C. L., and Ledwith, B. J. (1997). Peroxisome proliferators activate extracellular signal-regulated kinases in immortalized mouse liver cells. *J. Biol. Chem.* **272,** 13452–13457.
35. Passilly-Degrace, P., Jannin, B., Boscoboinik, D., Motojima, K., and Latruffe, N. (2000). Cipofibrate stimulates protein kinase C-dependent phosphorylation of an 85 kDa protein in rat Fao hepatic derived cells. *Biochimie* **82,** 749–753.
36. Nakai, K., and Kanehisa, M. (1992). A knowledge base for predicting protein localization sites in eukaryotic cells. *Genomics* **14,** 897–911.
37. Nishimaki-Mogami, T., Suzuki, K., Okochi, E., and Takahashi, A. (1996). Bezafibrate and clofibric acid are novel inhibitors of phosphatidylcholine synthesis via the methylation of phosphatidylethanolamine. *Biochim. Biophys. Acta* **1304,** 11–20.
38. Cui, Z., Vance, J. E., Chen. M. H., Voelker, D. R., and Vance, D. E. (1993). Cloning and expression of a novel phosphatidylethanolamine *N*-methyltransferase. A specific biochemical and cytological marker for a unique membrane fraction in liver. *J. Biol. Chem.* **268,** 16655–16663.
39. Nishimaki-Mogami, T., Suzuki, K., and Takahashi, A. (1996). The role of phosphatidylethanolamine methylation in the secretion of very low density lipoproteins by cultured rat hepatocytes: Rapid inhibition of phosphatidylethanolamine methylation by bezafibrate increases the density of apolipoprotein B48-containing lipoproteins. *Biochim. Biophys. Acta* **1304,** 21–31.
40. Cui, Z., Houweling, M., and Vance, D. E. (1995). Expression of phosphatidylethanolamine *N*-methyltransferase-2 in McArdle-RH7777 hepatoma cells inhibits the CDP-choline pathway for phosphatidylcholine biosynthesis via decreased gene expression of CTP:phosphocholine cytidylyltransferase. *Biochem. J.* **312,** 939–945.
41. Vance, D. E., and Ridgway, N. D. (1988). The methylation of phosphatidylethanolamine. *Prog. Lipid Res.* **27,** 61–79.
42. Kasurinen, J., van Paridon, P. A., Wirtz, K. W. A., and Somerharju, P. (1990). Affinity of phosphatidylcholine molecular species for the bovine phosphatidylcholine and phosphatidylinositol transfer proteins. Properties of the *sn*-1 and *sn*-2 acyl binding sites. *Biochemistry* **29,** 8548–8554.
43. Momchilova, A., Markovska, T., and Pankov, R. (1998). Phospholipid dependence of membrane-bound phospholipase A2 in ras-transformed NIH 3T3 fibroblasts. *Biochimie* **80,** 1055–1062.
44. Stillwell, W., Jenski, L. J., Crump, F. T., and Ehringer, W. (1997). Effect of docosahexaenoic acid on mouse mitochondrial membrane properties. *Lipids* **32,** 497–506.
45. Pehowich, D. J. (1999). Thyroid hormone status and membrane *n*-3 fatty acid content influence mitochondrial proton leak. *Biochim. Biophys. Acta* **1411,** 192–200.
46. Chavez, E., Moreno-Sanchez, R., Zazueta, C., Cuellar, A., Ramirez, J., Reyes-Vivas, H., Bravo, C., and Rodriguez-Enriquez, S. (1996). On the mechanism by which 6-ketocholestanol protects mitochondria against uncoupling-induced Ca^{2+} efflux. *FEBS Lett.* **379,** 305–308.
47. Niot, I., Gresti, J., Boichot, J., Sempore, G., Durand, G., Bezard, J., and Clouet, P. (1994). Effect of dietary n-3 and n-6 polyunsaturated fatty acids on lipid-metabolizing enzymes in obese rat liver. *Lipids* **29,** 481–489.

48. Paradies, G., Ruggiero, F. M., Petrosillo, G., and Quagliariello, E. (1997). Alterations in carnitine-acylcarnitine translocase activity and in phospholipid composition in heart mitochondria from hypothyroid rats. *Biochim. Biophys. Acta* **1362,** 193–200.

49. Paradies, G., and Ruggiero, F. M. (1989). Decreased activity of the pyruvate translocator and changes in the lipid composition of heart mitochondria from hypothyroid rats. *Arch. Biochem. Biophys.* **269,** 595–602.

50. Paradies, G., and Ruggiero, F. M. (1990). Age-related changes in the activity of the pyruvate carrier and in the lipid composition of rat-heart mitochondria. *Biochim. Biophys. Acta* **1016,** 207–212.

51. Froyland, L., Madsen, L., Vaagenes, H., Totland, G. K., Auwerx, J., Kryvi, H., Staels, B., and Berge, R. K. (1997). Mitochondrion is the principal target for nutritional and pharmacological control of triglyceride metabolism. *J. Lipid Res.* **38,** 1851–1858.

Received June 26, 2001
Revised version received November 28, 2001
Published online January 30, 2002